Automotive Experiences
Vol. 7 No. 1 (2024) pp. 86-96
p-ISSN: 2615-6202 e-ISSN: 2615-6636

Research Paper

Performance of Transition Metal Supported Al_2O_3 Coated on Honeycomb Catalysts and Its Segmentation on Exhaust Gasses Oxidation

Haris Puspito Buwono[1,2,3], **Hangga Wicaksana**[1,2], **Moh. Hartono**[1,2], **Joko Waluyo**[4], **Moch. Fauzun Daroini**[1], **Ilham Taufik Muslim**[1], **Masato Machida**[5]

[1] Department of Mechanical Engineering, Politeknik Negeri Malang, Lowokwaru, Malang 65141, Indonesia
[2] Center of Manufacture Research, Politeknik Negeri Malang, Lowokwaru, Malang 65141, Indonesia
[3] Center of Innovation and Integrated Technology Research, Politeknik Negeri Malang, Lowokwaru, Malang 65141, Indonesia
[4] Department of Chemical Engineering, Universitas Sebelas Maret, Jebres, Surakarta 57126, Indonesia
[5] Division of Materials Science and Chemistry, Faculty of Advanced Science and Technology, Kumamoto University, 2-39-1 Kurokami, Chuo, Kumamoto 860-8555, Japan

haris.puspito@polinema.ac.id

https://doi.org/10.31603/ae.10686

Published by Automotive Laboratory of Universitas Muhammadiyah Magelang

Article Info
Submitted: 15/12/2023
Revised: 05/04/2024
Accepted: 05/04/2024
Online first: 27/04/2024

Abstract

The oxidation of carbon monoxide (CO) and unburnt hydrocarbons (HC) under segmented honeycomb catalysts was investigated using actual exhaust gas mixtures from a gasoline-fueled internal combustion engine of a motorcycle. The honeycomb catalysts were prepared through a wet process, resulting in four types coated with transition metals (Cu, Cr, Fe, and Ni) supported on Al_2O_3. The oxidation of CO and HC was monitored using an exhaust gas analyzer across a range of air-to-fuel ratios (AFR), from lean to rich, under stationary conditions. The results demonstrate that the honeycomb catalysts effectively decreased CO and HC concentrations in the exhaust gas. Among the transition metal oxide honeycomb catalysts, Cr and Ni exhibited high CO and HC conversion rates, surpassing those observed with Cu. The average CO and HC conversion calculations, spanning from lean to rich air-to-fuel ratios, were consistent with the actual conversion rates achieved. Furthermore, the study investigated the effect of honeycomb segmentation on CO and HC conversion. Surprisingly, the catalytic performance of Cr and Ni remained high even with longer gaps in the honeycomb. Interestingly, the conversion of CO and HC over the iron oxide honeycomb catalyst increased as the gap in the honeycomb became longer. This is likely due to an increase in the gap size and enhanced re-mixing of reactants (CO, HC, and O_2) caused by recirculation. Thus, this study provides valuable elucidation on the potential application of segmented honeycomb catalysts for reducing CO and HC emissions in exhaust gases.

Keywords: Catalytic converter; Honeycomb; CO oxidation; HC oxidation; Segmentation; Transition metal

1. Introduction

Internal engine combustion produces carbon monoxide (CO) and unburnt hydrocarbon (HC) as byproducts of incomplete combustion, contributing to harmful emissions [1]–[3]. This contrasts with the advantages of low-temperature combustion and less NOx emission [4]–[6]. To mitigate this issue, catalysts are applied to convert CO and HC into less harmful carbon dioxide (CO_2) and water (H_2O) [7]. Conventionally, noble metals such as rhodium, platinum, and palladium have been used due to their high performance in oxidizing CO and volatile organic compounds (VOCs) [8]–[15]. However, their limited availability and high cost have slowed down their

widespread use in commercial processes [4], [8], [10], [12], [16].

In recent years, transition metal oxides have emerged as promising substitutes to noble metals for CO, HC, and VOC oxidation, offering advantages such as lower cost and comparable catalytic performance. Notably, cobalt, iron, copper, and nickel oxides supported on Al_2O_3 catalysts have demonstrated promising performance in CO, and HC oxidation, reducing the need for noble metal loading. This, in turn, contributes to a more economically attractive option [17]–[21].

Chromium oxide (CrO and Cr_2O_3) catalysts have shown high activity, selectivity, and thermal stability in CO oxidation [17]–[21]. The thin film of Cr_2O_3 with O_2 vacancies allows for CO adsorption on Cr^+ species surface or possibly on Cr_2O_3 interface sites, while O_2 interacts with Cr atoms to preserve the Cr_2O_3. This results in highly dispersed Cr_2O_3, and is advantageous for low-temperature CO oxidation. Various metal ions can be added into hexagonal Cr_2O_3 [18]. Similarly, copper oxide catalysts have shown efficient oxidation of CO. VOCs, and NH3 when supported on CeO_2 or Al_2O_3 [4], [22]–[29].

Nickel catalysts have been intensively investigated for CO oxidation. The catalytic activity of nickel is influenced by crystallite size, surface area, and pore volume. The catalytic activity of nickel for CO oxidation depends on its shapes consecutively is nanorods > nanobelt > nanowires > nanoflowers > nanospheres > nanocubes [30]–[32]. Moreover, nickel oxide is active in oxidizing hydrocarbons such as benzene, pentane, n-hexane, and formaldehyde [33], [34]. Iron oxide has also shown interesting CO oxidation capabilities even at ambient conditions. The catalytic activity of iron oxide nanoparticles for CO oxidation depends on particle size, surface area, surface-coordination unsaturated sites, and the concentration of hydroxyl groups [34]–[36].

In pursuit of higher catalytic activity, multi-segment catalysts with gaps between segments have been explored. This approach combines hetero- and homogenous reactions, enhancing HC conversion. In contrast, conventional catalytic combustion involves competition between these reactions [37]. Many studies have successfully explained the honeycomb catalyst gap in microreactors [37]–[41]. It has been demonstrated that multi-segment catalysts outperform single catalysts in hydrogen combustion, with longer gaps promoting homogeneous reactions, resulting in high reactant conversion over short distances [39]. High conversion rates of CO_2 methanation and CH_4 conversion are achieved with a longer catalyst gap while maintaining high selectivity, enabling efficient conversion over short distances [37], [40]. The gap in the segmented honeycombs facilitates a pre-reaction in an upstream catalyst segment, generating intermediates and catalytically inducing exothermicity [37].

Based on significant findings of transition metal oxides and catalysts segmentation, our study focuses on the practical application of honeycomb-shaped catalysts in exhaust systems. We prepared honeycomb catalysts using Cu, Cr, Fe, and Ni supported on Al_2O_3. The performance of these honeycomb catalysts was evaluated for CO and HC conversion using actual exhaust gas from gasoline internal combustion engines. Furthermore, we investigated the effects of segmentation gaps in the honeycomb catalysts on the catalytic activity of CO and HC conversion.

2. Materials and Method

2.1. *Catalyst Preparation*

Alumina (Al_2O_3) was prepared via a wet process. Aluminum sulfate was precipitated by 25 wt% ammonia under vigorous stirring. The precipitated was collected, washed, dried, and calcinated at 500 °C for 3 hours in the air. Subsequently, an aqueous solution of $CuCl_2$, CrO_3, $FeCl_3$, or $NiCl_2$ was impregnated onto the alumina, followed by drying, and calcination at 500 °C for 6 hours in air. The loading of transition metals on Al_2O_3 was 10 wt%. So, four types of catalysts were prepared, namely Cu/Al_2O_3, Cr/Al_2O_3, Fe/Al_2O_3, and Ni/Al_2O_3.

In this study, four types of honeycomb-coated catalysts were prepared. The powder of Cu/Al_2O_3, Cr/Al_2O_3, Fe/Al_2O_3, and Ni/Al_2O_3 catalysts was coated onto a monolith honeycomb as illustrated in **Figure 1**. The monolith honeycomb catalysts were prepared by immersing a honeycomb (2.5 mm in diameter × 30 mm, 69 cells) into a slurry prepared with 30 wt% catalyst powders, and water. Subsequently, the coated honeycomb was dried at 100 °C and calcined in the air at 500 °C for 3 hours.

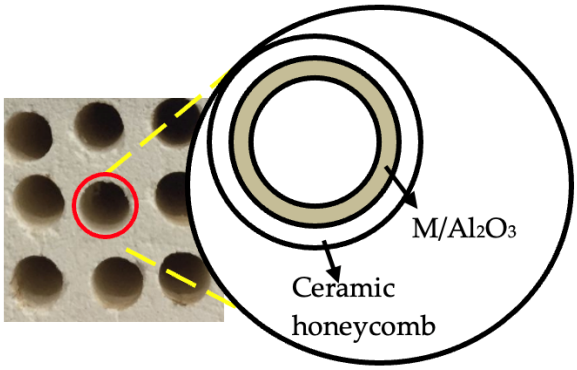

Figure 1. Schematic illustration of honeycomb catalysts. M means transition metals of Cu, Cr, Fe, or Ni

2.2. *Catalytic Performance Testing*

The catalytic activity evaluation of the honeycomb catalysts was conducted within an exhaust gas system of a gasoline-fueled internal combustion engine, specifically from a motorcycle. The system employed a flow reactor configuration, with the honeycomb catalysts positioned at a distance of 40 cm from the combustion chamber. Testing was conducted under stationary conditions, wherein the motorcycle remained fixed in place.

Initially, data collection began over fresh catalysts after the engine was started from a cold state and allowed to run for 10 minutes at 1500 rpm. Subsequently, data were collected incrementally as the engine rotation speeds varied from 1500 to 7500 rpm. Throughout the experiment, the exhaust gases were maintained under steady-state conditions.

The honeycomb catalysts featured a gap ranging from 1 to 3 cm, as shown in **Figure 2**. The concentration of CO and HCs in the effluent gas stream was monitored using a gas analyzer.

3. Results and Discussion

3.1. *Actual Exhaust Gasses*

Table 1 presents the actual exhaust gas composition of a gasoline-fueled internal combustion engine from a motorcycle, observed without the presence of a honeycomb catalyst. The data confirms that as the engine rotation speed increases, the concentration of CO rises, while the concentration of HC decreases. Conversely, the concentrations of CO_2 and O_2 increase with higher engine rotation speeds. This trend can be explained

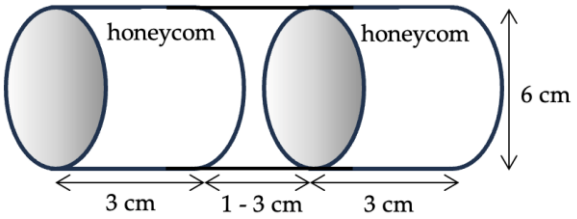

Figure 2. Schematic illustration of honeycomb catalysts arrangement. The gap of the honeycomb catalyst was 1 – 3 cm

by the increased flow rate of fuel as the engine rotation speed rises, while the flow rate of air remains relatively constant. At elevated engine rotation speeds (6500 rpm), incomplete combustion of the fuel-air mixture within the engine cylinders is likely, resulting in higher levels of unburned fuel, including CO, in the exhaust gases compared to lower engine speeds (5500 rpm). Consequently, the conversion of CO decreases. This phenomenon results in the air-to-fuel ratio (AFR) becoming richer at higher engine rotation speeds and leaner at lower engine rotation speeds.

Figure 3 further illustrates these observations, depicting the correlation between AFR and lambda as a function of engine rotation speed. The AFR values range from 14.1 to 19.6, indicating that the experiments were conducted under both reducing and oxidizing conditions, depending on the engine rotation speed. The shift of the AFR from lean to rich condition with increasing engine rotation speeds aligns with Eq. 1, which describes AFR as a function of the mass ratio of air to fuel. According to Eq. 1, as the mass of air remains constant and the mass of fuel increases, the AFR decreases. This decrease in AFR explains the transition towards richer conditions at higher engine rotation speeds.

Overall, these results provide a valuable understanding of the exhaust gas composition of the gasoline engine without a honeycomb catalyst at different engine rotation speeds. Understanding the correlation between engine rotation speed, AFR, and exhaust gas composition is essential for evaluating the effectiveness of honeycomb catalytic converters in reducing harmful emissions.

$$AFR = \frac{mass_{air}}{mass_{fuel}} \quad (1)$$

Table 1. Actual exhaust gas composition of a gasoline-fueled internal combustion engine of a motorcycle in the absence of a honeycomb catalyst

Engine speed (rpm)	CO (%)	HC (ppm)
1500	3.95	531
2500	3.94	533
3500	4.52	273
4500	4.26	305
5500	5.38	144
6500	4.30	157
7500	5.38	144

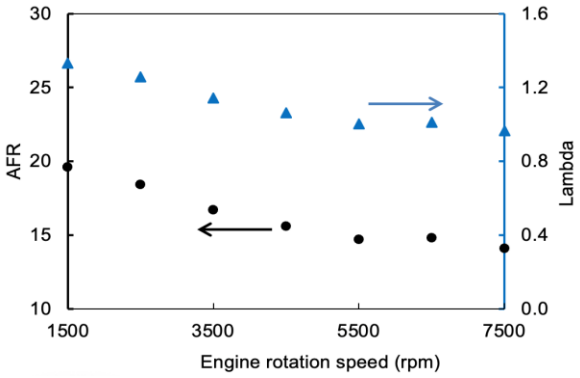

Figure 3. The correlation between engine rotation speed towards AFR and lambda (λ)

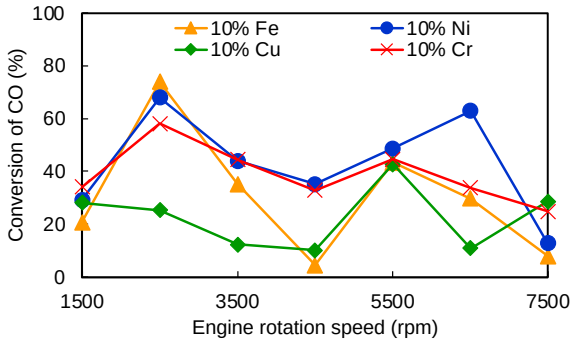

Figure 4. The catalytic activity of CO conversion for four honeycomb-supported catalysts, with a gap of 1 cm between honeycombs

3.2. *Catalytic Activity*

Figure 4 shows the catalytic performance of CO conversion for four types of honeycomb catalysts featuring metal oxide catalysts, including Cu, Cr, Fe, and Ni, supported on Al_2O_3 with a gap of 1 cm between honeycombs. The results demonstrate dynamic CO conversion rates across different engine rotation speeds for all honeycomb catalysts. However, nickel and chromium oxide catalysts consistently exhibit high CO conversion rates across all engine rotation speeds or AFRs, whereas iron and copper oxide catalysts show comparatively lower CO conversion rates. The observed trends suggest that the catalytic activity order for CO conversion in honeycomb catalysts is as follows: Ni > Cr > Fe > Cu, with nickel oxide demonstrating the highest CO conversion rate and copper oxide displaying the lowest CO conversion rate among the tested catalysts.

Figure 5 shows the catalytic activity of HC conversion for the same four types of honeycomb catalysts coated with transition metals (Cu, Cr, Fe, and Ni) supported on Al_2O_3, with a gap of 1 cm between honeycombs. Similar to CO conversion, the results indicate dynamic HC conversion rates at different engine rotation speeds. However, only chromium oxide catalysts consistently demonstrated high HC conversion for all engine

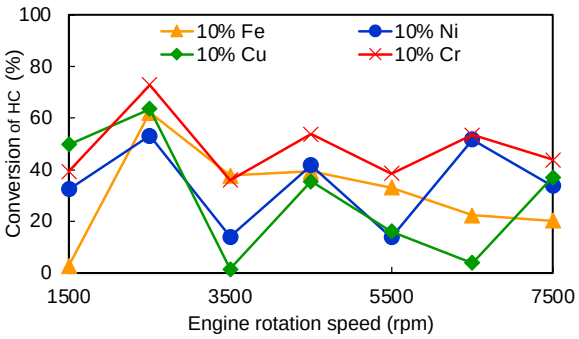

Figure 5. The catalytic activity of HC conversion for four honeycomb catalysts coated with transition metal (including Cu, Cr, Fe, and Ni) supported Al_2O_3, with a gap of 1 cm between honeycombs

rotation speeds or AFRs, while copper oxide showed lower HC conversion. The catalytic activity order for HC conversion was as follows: Cr > Ni = Fe > Cu, with chromium oxide displaying the highest HC conversion, whereas copper oxide showed lower HC conversion on a honeycomb catalyst.

These findings highlight the varying catalytic performances of the different honeycomb catalysts coated with transition metals (Cu, Cr, Fe, and Ni) supported on Al_2O_3 for CO and HC conversion. The nickel and chromium oxide catalysts consistently showed superior CO

conversion, while chromium oxide demonstrated high HC conversion. Conversely, iron and copper oxide catalysts showed lower conversion rates for both CO and HC. The reasons for the zigzagging pattern in the catalytic activity of CO and HC conversion among four different honeycomb-supported catalysts (Cu, Cr, Ni, and Fe) remain unclear. Further investigation is needed to comprehensively understand the underlying mechanisms driving this observed behavior.

Given the dynamic results observed for CO and HC conversion, determining which catalyst exhibits better overall catalytic performance for a motorcycle operating under varying AFR conditions is challenging. Motorcycles typically operate across a range of AFRs, transitioning from lean to rich or vice versa, from rich to lean. Therefore, to address this, a simple model was developed based on the average conversion from lean to rich AFR. **Figure 6** shows the average catalytic activity of CO and HC conversion for different supported catalysts using this model. The results indicate that chromium and nickel oxide exhibited the highest CO conversion, while copper oxide showed lower CO conversion on the honeycomb catalyst. This simple model aims to represent the actual CO and HC conversion data obtained at different engine rotation speeds, which displayed dynamic conversion trends.

The catalytic activity order for CO conversion in honeycomb catalysts was determined as Ni > Cr > Fe > Cu, indicating that nickel achieved the highest CO conversion among the tested catalysts. This result is consistent with the known catalytic performance order of supported base metal oxide transition catalysts of single transition metals, except for iron oxide. The catalytic activity of CO oxidations order of supported base metal oxide

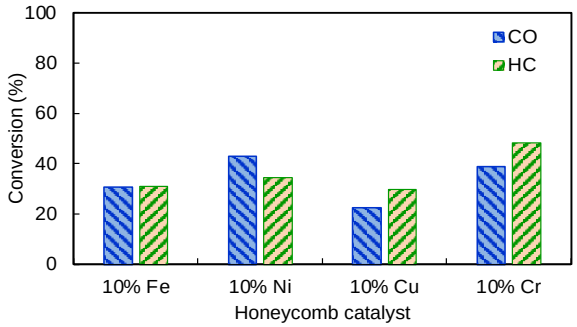

Figure 6. The average catalytic activity for the simplicity of CO and HC conversion of four different supported catalysts

transition catalysts of single transition metal is reposted as Co_3O_4 > Cu_2O > Fe_2O_3 > NiO > Cr_2O_3 [42]. Since this experiment utilized $CuCl_2$, CrO_3, $FeCl_3$, or $NiCl_2$ precursors, the transition metal oxides present were CuO, CrO_3, Fe_2O_3, and NiO. In this study, iron (II) oxide was found to be less active than NiO. The exact reason remained unclear, but the presence of sulfate in the catalyst support precursor may have influenced the catalytic activity. Studies by Çılgı and Cetişli and Buwono et al. have shown that the presence of sulfate in the precursor remains constant below calcination at 800 °C and could decrease the amount of active metal on the catalyst surface, resulting in decreased catalytic performance [43], [44]. In contrast, the high catalytic performance of Fe_2O_3 over alumina for CO oxidation was observed when prepared using a chemical vapor deposition method [35]. According to Dey and Mehta, the oxidation of carbon monoxide (CO) is strongly affected by the size of the crystals in nickel oxide catalysts. When the crystal size of the catalyst decreases, the CO oxidation rate increases until it reaches a certain point. However, beyond this point, further reduction in crystal size leads to a decrease in the conversion of CO oxidation [31]. Therefore, it is reasonable to suggest that the preparation method affects the crystal size, which in turn can influence the catalytic performance of the catalyst material.

The catalytic activity order for HC conversion was determined as Cr > Ni > Fe > Cu, with chromium (Cr) achieving the highest conversion rate among the honeycomb catalysts. This result is consistent with the known catalytic performance order of supported base metal oxide transition catalysts of single transition metals. The high catalytic activity of chromium catalysts in HC conversion may be attributed to the presence of both Cr^{3+} and Cr^{6+} species after calcination, as explained by Sainio et al. [45]. They utilized CrO_3 as the precursor, and X-ray Photoelectron Spectroscopy (XPS) analysis revealed the presence of Cr^{3+} and Cr^{6+} species after calcination. These species might have contributed to the high HC conversion observed in honeycomb catalysts.

Additionally, the HC conversion in honeycomb catalysts may have been influenced by the catalyst support (alumina), as seen in previous studies where the HC conversion order of unsupported base metal oxides differed from

that of metal oxides supported on alumina [34]. For instance, unsupported base metal oxides exhibited HC conversion order, from high to low, of cobalt-, manganese-, nickel-, and iron-oxide. However, the presence of support changed the order of catalytic activity with metal oxides supported on alumina showing an HC conversion order of manganese oxide, chromium oxide, and cobalt oxide [34]. This suggests that alumina as a supported catalyst plays a role in affecting the HC conversion, leading to different catalytic performances compared to unsupported catalysts. Furthermore, the phenomenon of strong metal-support interaction (SMSI) may have also influenced catalytic activity. Elevated temperatures can cause the support to cover the active metal so that reducing the number of active catalytic sites [46]. This interaction could further contribute to variations in the catalytic activity of the supported catalysts.

In brief, the experimental findings highlight the varying catalytic activities of the honeycomb catalysts coated with transition metals (Cu, Cr, Fe, and Ni) supported Al_2O_3 for CO and HC conversion. Nickel oxide exhibited the highest CO conversion, while chromium oxide demonstrated the highest HC conversion. However, the exact reason for these observed differences in catalytic activities remains elusive but may be linked to factors such as electronic structure, oxygen mobility surface species, and active sites. Another reason is probably related to the resilience of metal towards sulfate content as support precursors and chlorine from metal salts. The presence of sulfate in the precursor, along with phenomena like strong metal-support interaction (SMSI), might have influenced the catalytic activities of the supported catalysts, resulting in variations in catalytic performances compared to unsupported catalysts.

3.3. *Honeycomb Catalyst Segmentation*

Moreover, to elucidate the effect of the gap between honeycomb, catalyst segmentation was performed. **Figure 7** and **Figure 8** provide insights into the influence of the gap between honeycombs on CO and HC conversion for various types of honeycomb catalysts coated with transition metal (Cu, Cr, Fe, and Ni) supported on Al_2O_3, with gap sizes ranging from 1 to 3 cm. **Figure 7** demonstrates that, in general, as the gap between honeycombs widens, the CO conversion decreases for most of the tested catalysts. However, an interesting exception is observed with the iron oxide honeycomb catalyst, where CO conversion increases as the gap widens. This demonstrates that the gap has an important effect on the catalytic activity of the honeycomb catalysts, and the effect varies depending on the specific metal oxide catalyst used. Similarly, **Figure 8** demonstrates the effect of the honeycomb gap on HC conversion. In most cases, as the gap increases, HC conversion decreases for the tested honeycomb catalysts. However, both the iron- and nickel-oxide honeycomb catalysts exhibit the opposite trend, where both CO and HC conversion rates increase as the gap widens. With a longer gap, there is more space for the exhaust gases to mix and flow before reaching the catalyst-coated portions of the honeycomb. This potential improvement in dispersion ensures a more uniform distribution over the catalyst surface, thereby enhancing conversion efficiency. Consequently, enhanced mixing and flow facilitate a more efficient conversion of CO and

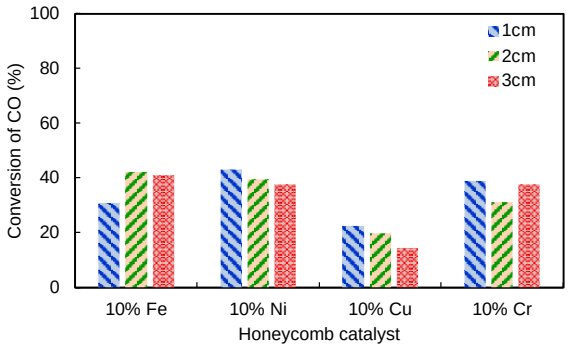

Figure 7. The average catalytic activity of CO conversion for different supported honeycomb catalysts with a gap of 1 – 3 cm

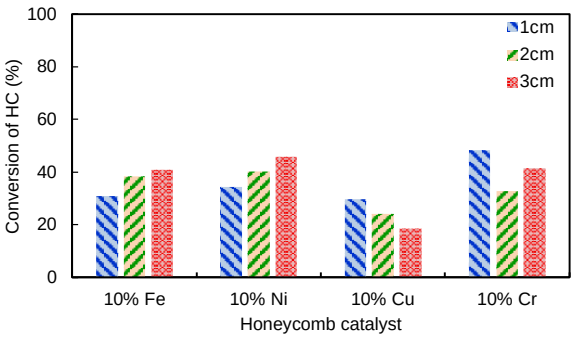

Figure 8. The average catalytic activity of HC conversion for different honeycomb-supported catalysts with a gap of 1 – 3 cm

HC into less harmful byproducts. This highlights the complex interplay between the gap and the catalytic activity of different metal oxide catalysts.

The findings emphasize the importance of catalyst segmentation and the role of the gap between honeycombs in influencing CO and HC conversion rates. The CO and HC oxidation reactions involve a collaborative mechanism between hetero- and homogeneous reactions. The pre-reaction of the heterogeneous reaction on the first honeycomb catalyst assists the second homogeneous reaction by providing the necessary catalytically induced exothermicity. This cooperative behavior has been supported by previous studies. For instance, Li et al. demonstrated that the second catalyst segment promotes the reduction of CO due to its high adherence coefficient on the platinum surface, leading to high CH_4 conversion and complete oxidation in a short distance [37].

Another factor contributing to the varying catalytic performance of honeycomb catalysts can be addressed to the different catalyst behavior, flow conditions, and different reactor properties associated with multi-segment catalysts [37], [41]. **Figure 9** illustrates the vector of velocity and pressure of honeycomb catalysts as a function of the gap, ranging from 1 to 3 cm. When the gap is 1 cm (**Figure 9a**), the velocity vector within the gap tends to remain relatively constant, as indicated by the red color. However, as the gap increases to 2 and 3 cm, (**Figure 9b** and **Figure 9c**, respectively), the velocity vector within the gap tends to decrease, represented by the green color. Additionally, the vectors in the gap of 3 cm show a spreading out phenomenon, leading to recirculation within the gap in contrast to those observed in the 1cm gap.

This decrease in velocity with increasing gap size is in accordance with the principle of mass conservation. As the gap widens, the cross-sectional area of the pipe increases, resulting in a decrease in velocity while maintaining constant mass flow. The tendency of fluids to fill the space between gaps is particularly evident in **Figure 9c**. The change in fluid direction and increased vorticity contribute to higher pressure at the end of the gap zone, potentially causing pressure drops in the fluids. Upon entering the second honeycomb hole, the cross-sectional area of the pipe decreases, leading to an increase in fluid velocity while adhering to the law of mass conservation. Furthermore, the recirculation of reactants (CO, HC, and O_2) within the honeycomb catalyst gap promotes better mixing of the reactants. Enhanced mixing facilitates additional opportunities for reactant molecules to interact with active sites on the catalyst surface, thereby promoting catalytic reactions.

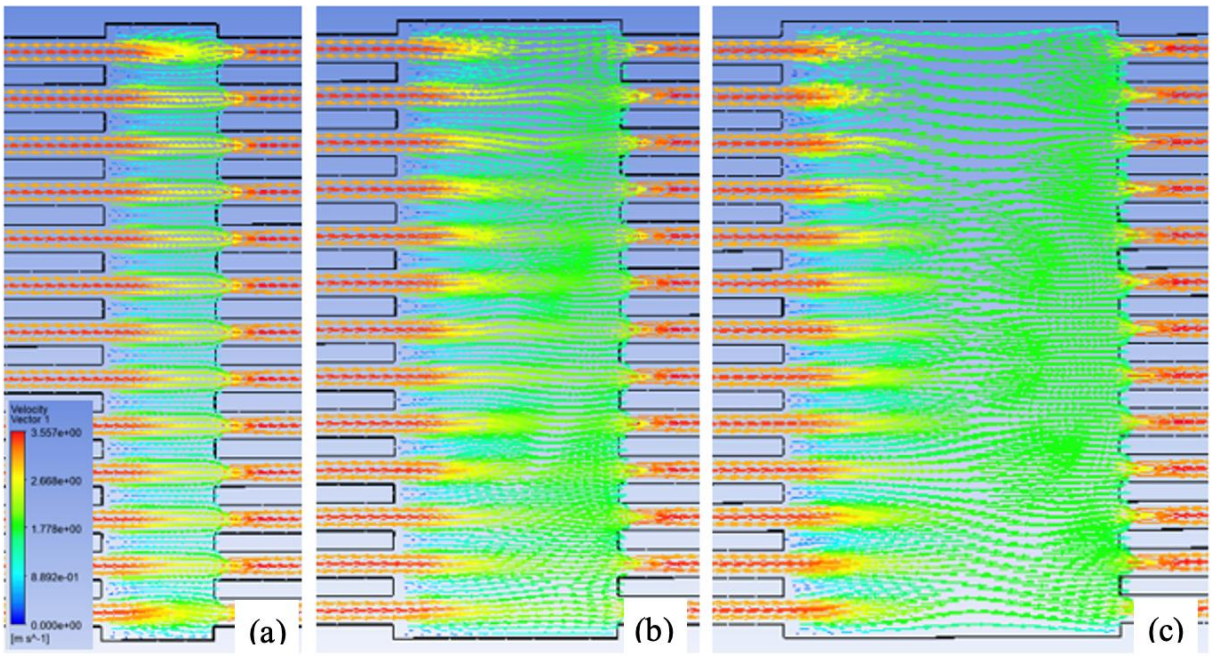

Figure 9. The velocity vector of honeycomb catalysts as a function of the gap, ranging from 1 (a), 2 (b), and 3 cm (c)

It is well known that the efficient mixing of the reactants increases the probability of collisions between the reactant molecules and the catalyst, thereby leading to the catalytic reaction. This enhanced mixing and re-mixing of the reactants within the gap of the honeycomb catalyst can lead to improved reaction rates and overall catalytic performance. In some cases, the gap did not increase catalytic performance. These phenomena are probably related to high reaction rates, in line with as observed by Chen et al. [39]. For example, in the case of Fe/Al_2O_3 supported on honeycomb, an increase in the honeycomb gap led to increased CO and HC conversion rates. This could be attributed to improved mass transport and enhanced access of reactants to catalytic sites, thereby boosting the catalytic activity of Fe/Al_2O_3 in CO and HC oxidation reactions. The enhanced mass transport may also facilitate better oxygen supply to the catalyst surface, thereby facilitating redox processes and resulting in higher CO and HC conversion rates.

In contrast, Cu, Cr, and Ni catalysts supported on honeycomb may already possess effective oxygen activation and are less affected by changes in mass transport by a gap. Copper (Cu) is highly efficient in low-temperature oxidation, Chromium (Cr) may not exhibit a direct correlation between the gap and catalytic activity in CO and HC oxidation, as it can be more selective in different oxidation reactions. Nickel (Ni) is generally more active in steam reforming, rather than in CO and HC oxidation. Overall, the recirculation and re-mixing of reactants within the honeycomb catalyst's gap play a crucial role in enhancing the catalytic performance and optimizing the efficiency of CO and HC conversion processes. However, the specific impact of the gap size on catalytic performance may vary depending on the catalyst type and its inherent properties.

4. Conclusion

Four different honeycomb-coated catalysts containing Al_2O_3 as support for Cr, Ni, Fe, and Cu were prepared, and their catalytic performances under actual CO and HC oxidation conditions were studied compared to standard conditions (without catalyst). The catalyst's performance was evaluated based on catalytic conversion rates. Notably, all four honeycomb catalysts effectively decreased the concentration of CO and HC in the exhaust gas. High CO and HC conversion were achieved by Cr, Fe, and Ni, with the catalytic activity order as follows: Cr ≥ Ni > Fe > Cu. Furthermore, the study explored the impact of honeycomb segmentation. Interestingly, as the gap of the honeycomb increased, both Cr and Ni catalysts maintained their high catalytic efficiency for CO and HC conversion rates. Remarkably, the iron oxide honeycomb catalyst displayed an increase in both the CO and HC conversion, while the nickel oxide honeycomb catalyst showed an increase in the HC conversion. The gap facilitates the recirculation and re-mixing of reactants within the honeycomb catalyst, which is important for improving catalytic performance and optimizing the efficiency of CO and HC conversion processes. The findings call attention to the importance of catalyst composition and segmentation in improving the conversion of different exhaust gases. Further research in this area could lead to advancements in emission control technology for oxidation.

Acknowledgements

This study was supported by Politeknik Negeri Malang.

Author's Declaration

Authors' contributions and responsibilities

The authors made substantial contributions to the conception and design of the study. The authors took responsibility for data analysis, interpretation and discussion of results. The authors read and approved the final manuscript.

Funding

No funding information from the authors

Availability of data and materials

All data are available from the authors.

Competing interests

The authorsdeclare no competing interest.

Additional information

No additional information from the authors.

References

[1] W. Purwanto, J. C. T. Su, M. L. Rochman, B. Waluyo, K. Krismadinata, and A. Arif, "Study on the Addition of A Swirling Vane to Spark Ignition Engines Fueled by Gasoline and Gasoline-Ethanol," *Automotive*

Experiences, vol. 6, no. 1, pp. 162–172, 2023, doi: https://doi.org/10.31603/ae.7981.

[2] M. Hanifuddin, M. F. Taufiqurrahman, T. A. Setyawan, R. Anggarani, C. S. Wibowo, and B. Sugiarto, "Performance of a Single-Cylinder Four-Stroke Engine with High Concentrations of Gasoline-Ethanol-Methanol (GEM)," *Automotive Experiences*, vol. 6, no. 2, pp. 407–415, Aug. 2023, doi: 10.31603/ae.9332.

[3] B. Sulistyo, H. Sofyan, T. Sukardi, and A. Widyianto, "Performance and Emission Characteristics Using Dual Injection System of Gasoline and Ethanol," *Automotive Experiences*, vol. 6, no. 2, pp. 245–258, May 2023, doi: 10.31603/ae.8070.

[4] I. Heo, M. H. Wiebenga, J. R. Gaudet, I. S. Nam, W. Li, and C. H. Kim, "Ultra low temperature CO and HC oxidation over Cu-based mixed oxides for future automotive applications," *Applied Catalysis B: Environmental*, vol. 160–161, no. 1, pp. 365–373, 2014, doi: 10.1016/j.apcatb.2014.05.045.

[5] D. Han, A. M. Ickes, S. V. Bohac, Z. Huang, and D. N. Assanis, "HC and CO emissions of premixed low-temperature combustion fueled by blends of diesel and gasoline," *Fuel*, vol. 99, no. September, pp. 13–19, 2012, doi: 10.1016/j.fuel.2012.04.010.

[6] K. D. Cung, S. A. Ciatti, S. Tanov, and Ö. Andersson, "Low-Temperature Combustion of High Octane Fuels in a Gasoline Compression Ignition Engine," *Frontiers in Mechanical Engineering*, vol. 3, no. December, pp. 1–14, 2017, doi: 10.3389/fmech.2017.00022.

[7] S. R. Ariyanto, S. Suprayitno, and R. Wulandari, "Design of Metallic Catalytic Converter using Pareto Optimization to Improve Engine Performance and Exhaust Emissions," *Automotive Experiences*, vol. 6, no. 1, pp. 200–2015, Apr. 2023, doi: 10.31603/ae.7977.

[8] H. S. Gandhi, G. W. Graham, and R. W. McCabe, "Automotive exhaust catalysis," *Journal of Catalysis*, vol. 216, no. 1–2, pp. 433–442, 2003, doi: 10.1016/S0021-9517(02)00067-2.

[9] A. Gremminger, J. Pihl, M. Casapu, J. D. Grunwaldt, T. J. Toops, and O. Deutschmann, "PGM based catalysts for exhaust-gas after-treatment under typical diesel, gasoline and gas engine conditions with focus on methane and formaldehyde oxidation," *Applied Catalysis B: Environmental*, vol. 265, 2020, doi: 10.1016/j.apcatb.2019.118571.

[10] H. Tanaka, H. Fujikawa, and I. Takahashi, "Excellent Oxygen Storage Capacity of Perovskite-PD Three way Catalysts," *Applied Catalysis A: General*, vol. 39, no. 412, pp. 5051–5066, Aug. 1995, doi: 10.4271/950256.

[11] H. P. Buwono *et al.*, "Lean NOx reduction over Rh/ZrP2O7 catalyst under steady-state and perturbation conditions," *Catalysis Today*, vol. 281, no. x, pp. 583–589, 2017, doi: 10.1016/j.cattod.2016.05.020.

[12] H. P. Buwono *et al.*, "Rh Supported on LaPO4/SiO2 Nanocomposites as Thermally Stable Catalysts for TWC Applications," *Emission Control Science and Technology*, vol. 1, no. 4, pp. 284–291, 2015, doi: 10.1007/s40825-015-0024-9.

[13] Y. Nagao *et al.*, "Rh/ZrP2O7 as an efficient automotive catalyst for NOx reduction under slightly lean conditions," *ACS Catalysis*, vol. 5, no. 3, pp. 1986–1994, 2015, doi: 10.1021/cs5020157.

[14] H. L. Huynh and Z. Yu, "CO2 Methanation on Hydrotalcite-Derived Catalysts and Structured Reactors: A Review," *Energy Technology*, vol. 8, no. 5, 2020, doi: 10.1002/ente.201901475.

[15] H. Puspito Buwono *et al.*, "Enhanced Rh-anchoring on the composite metal phosphate Y0.33Zr2(PO4)3 in three-way catalysis," *Catalysis Science & Technology*, vol. 9, no. 19, pp. 5447–5455, 2019, doi: 10.1039/C9CY01274E.

[16] B. Agula, Q.-F. Deng, M.-L. Jia, Y. Liu, B. Zhaorigetu, and Z.-Y. Yuan, "Catalytic oxidation of CO and toluene over nanostructured mesoporous NiO/Ce0.8Zr0.2O2 catalysts," *Reaction Kinetics, Mechanisms and Catalysis*, vol. 103, no. 1, pp. 101–112, 2011, doi: 10.1007/s11144-011-0296-1.

[17] M. Cherian, M. S. Rao, W.-T. Yang, J.-M. Jehng, A. M. Hirt, and G. Deo, "Oxidative dehydrogenation of propane over

Cr2O3/Al2O3 and Cr2O3 catalysts: effects of loading, precursor and surface area," *Applied Catalysis A: General*, vol. 233, no. 1, pp. 21–33, 2002, doi: https://doi.org/10.1016/S0926-860X(02)00132-1.

[18] S. Dey and V. V. P. Kumar, "Supported and un-supported zinc and chromium oxide catalysts for lower temperature CO oxidation: A review," *Environmental Challenges*, vol. 3, no. February, p. 100061, 2021, doi: 10.1016/j.envc.2021.100061.

[19] R. C. Weast, Ed., *Handbook of Chemistry and Physics*. Boca Raton, Florida: Florida: CRC Press Inc., 1984.

[20] P. Michorczyk, J. Ogonowski, P. Kuśtrowski, and L. Chmielarz, "Chromium oxide supported on MCM-41 as a highly active and selective catalyst for dehydrogenation of propane with CO2," *Applied Catalysis A: General*, vol. 349, no. 1, pp. 62–69, 2008, doi: 10.1016/j.apcata.2008.07.008.

[21] X. Zhang, Y. Yue, and Z. Gao, "Chromium Oxide Supported on Mesoporous SBA-15 as Propane Dehydrogenation and Oxidative Dehydrogenation Catalysts," *Catalysis Letters*, vol. 83, no. 1, pp. 19–25, 2002, doi: 10.1023/A:1020693028720.

[22] M. Krämer, T. Schmidt, K. Stöwe, and W. F. Maier, "Structural and catalytic aspects of sol–gel derived copper manganese oxides as low-temperature CO oxidation catalyst," *Applied Catalysis A: General*, vol. 302, no. 2, pp. 257–263, 2006, doi: 10.1016/j.apcata.2006.01.018.

[23] Y. Bu, J. W. H. Niemantsverdriet, and H. O. A. Fredriksson, "Cu Model Catalyst Dynamics and CO Oxidation Kinetics Studied by Simultaneous in Situ UV-Vis and Mass Spectroscopy," *ACS Catalysis*, vol. 6, no. 5, pp. 2867–2876, 2016, doi: 10.1021/acscatal.5b02861.

[24] S. Dey, G. C. Dhal, R. Prasad, and D. Mohan, "Total oxidation of CO by CuMnOx catalyst at a low temperature," *International Journal of Scientific & Engineering Research*, vol. 7, no. 10, pp. 1730–1737, 2016.

[25] S. Dey, G. C. Dhal, R. Prasad, and D. Mohan, "Effect of nitrate metal (Ce, Cu, Mn and Co) precursors for the total oxidation of carbon monoxide," *Resource-Efficient Technologies*, vol. 3, no. 3, pp. 293–302, 2017, doi: 10.1016/j.reffit.2016.12.010.

[26] T.-J. Huang and D.-H. Tsai, "CO Oxidation Behavior of Copper and Copper Oxides," *Catalysis Letters*, vol. 87, no. 3, pp. 173–178, 2003, doi: 10.1023/A:1023495223738.

[27] D. Gamarra, C. Belver, M. Fernández-García, and A. Martínez-Arias, "Selective CO Oxidation in Excess H2 over Copper−Ceria Catalysts: Identification of Active Entities/Species," *Journal of the American Chemical Society*, vol. 129, no. 40, pp. 12064–12065, Oct. 2007, doi: 10.1021/ja073926g.

[28] C. L. Pitman *et al.*, "Stabilization of reduced copper on ceria aerogels for CO oxidation," *Nanoscale Advances*, vol. 2, no. 10, pp. 4547–4556, 2020, doi: 10.1039/d0na00594k.

[29] G. Ma, L. Wang, X. Wang, L. Li, and H. Ma, "CO Oxidation over Alumina-Supported Copper Catalysts," *Catalysts*, vol. 12, no. 9, 2022, doi: 10.3390/catal12091030.

[30] C. Maharaj, D. Lokhat, and R. Rawatlal, "Oxidation of carbon monoxide over supported nickel oxide catalyst: kinetic model development and identification," *South African Journal of Chemical Engineering*, vol. 39, no. November 2021, pp. 106–116, 2022, doi: 10.1016/j.sajce.2021.12.001.

[31] S. Dey and N. S. Mehta, "Oxidation of carbon monoxide over various nickel oxide catalysts in different conditions: A review," *Chemical Engineering Journal Advances*, vol. 1, no. June, p. 100008, 2020, doi: 10.1016/j.ceja.2020.100008.

[32] W. C. Conner and C. O. Bennett, "Carbon monoxide oxidation on nickel oxide," *Journal of Catalysis*, vol. 41, no. 1, pp. 30–39, 1976, doi: 10.1016/0021-9517(76)90197-4.

[33] J. J. Foster and R. I. Masel, "Formaldehyde oxidation on nickel oxide," *Industrial & Engineering Chemistry Product Research and Development*, vol. 25, no. 4, pp. 563–568, Dec. 1986, doi: 10.1021/i300024a010.

[34] K. C. Stein, J. J. Feenan, G. P. Thompson, J. F. Shultz, L. J. E. Hofer, and R. B. Anderson, "The oxidation of hydrocarbons on simple oxide catalysts," *Journal of the Air Pollution Control Association*, vol. 10, no. 4, pp. 275–281, 1960, doi: 10.1080/00022470.1960.10467930.

[35] I. H. Kim, H. O. Seo, E. J. Park, S. W. Han, and Y. D. Kim, "Low temperature CO oxidation over iron oxide nanoparticles decorating internal structures of a mesoporous alumina," *Scientific Reports*, vol. 7, no. January, pp. 1–11, 2017, doi: 10.1038/srep40497.

[36] H.-Y. Lin, Y.-W. Chen, and W.-J. Wang, "Preparation of nanosized iron oxide and its application in low temperature CO oxidation," *Journal of Nanoparticle Research*, vol. 7, no. 2, pp. 249–263, 2005, doi: 10.1007/s11051-005-4717-9.

[37] Y. H. Li, G. B. Chen, H. W. Hsu, and Y. C. Chao, "Enhancement of methane combustion in microchannels: Effects of catalyst segmentation and cavities," *Chemical Engineering Journal*, vol. 160, no. 2, pp. 715–722, 2010, doi: 10.1016/j.cej.2010.03.057.

[38] S. Ratchahat, M. Sudoh, Y. Suzuki, W. Kawasaki, R. Watanabe, and C. Fukuhara, "Development of a powerful CO2 methanation process using a structured Ni/CeO2 catalyst," *Journal of CO2 Utilization*, vol. 24, pp. 210–219, 2018, doi: 10.1016/j.jcou.2018.01.004.

[39] G. B. Chen, Y. C. Chao, and C. P. Chen, "Enhancement of hydrogen reaction in a micro-channel by catalyst segmentation," *International Journal of Hydrogen Energy*, vol. 33, no. 10, pp. 2586–2595, 2008, doi: 10.1016/j.ijhydene.2008.02.071.

[40] C. Fukuhara, Y. Suzuki, R. Watanabe, M. Sudoh, and S. Ratchahat, "Estimation of heat and mass transfer of structured catalyst system for CO 2 methanation .," in *The 25th International Symposium on Chemical Engineering Reaction*, 2018, pp. 4–5.

[41] Y.-H. Li, G.-B. Chen, F.-H. Wu, T.-S. Cheng, and Y.-C. Chao, "Effects of catalyst segmentation with cavities on combustion enhancement of blended fuels in a micro channel," *Combustion and Flame*, vol. 159, no. 4, pp. 1644–1651, 2012, doi: 10.1016/j.combustflame.2011.11.017.

[42] S. Dey and N. S. Mehta, "Automobile pollution control using catalysis," *Resources, Environment and Sustainability*, vol. 2, no. September, p. 100006, 2020, doi: 10.1016/j.resenv.2020.100006.

[43] G. K. Çılgı and H. Cetişli, "Thermal decomposition kinetics of aluminum sulfate hydrate," *Journal of Thermal Analysis and Calorimetry*, vol. 98, no. 3, pp. 855–861, 2009, doi: 10.1007/s10973-009-0389-5.

[44] H. P. Buwono, S. Minami, K. Uemura, and M. Machida, "Surface Properties of Rh/AlPO<inf>4</inf> Catalyst Providing High Resistance to Sulfur and Phosphorus Poisoning," *Industrial and Engineering Chemistry Research*, vol. 54, no. 29, pp. 7233–7240, 2015, doi: 10.1021/acs.iecr.5b01720.

[45] J. Sainio *et al.*, "An XPS study of CrOx on a thin alumina film and in alumina supported catalysts," *Applied Surface Science*, vol. 252, no. 4, pp. 1076–1083, 2005, doi: 10.1016/j.apsusc.2005.02.029.

[46] F. Polo-Garzon *et al.*, "In Situ Strong Metal–Support Interaction (SMSI) Affects Catalytic Alcohol Conversion," *ACS Catalysis*, vol. 11, no. 4, pp. 1938–1945, Feb. 2021, doi: 10.1021/acscatal.0c05324.